

SPDMark: Selective Parameter Displacement for Robust Video Watermarking

Samar Fares¹, Nurbek Tastan¹, Karthik Nandakumar^{1,2}

¹Mohamed bin Zayed University of Artificial Intelligence (MBZUAI), UAE

²Michigan State University (MSU), USA

Abstract

The advent of high-quality video generation models has amplified the need for robust watermarking schemes that can be used to reliably detect and track the provenance of generated videos. Existing video watermarking methods based on both post-hoc and in-generation approaches fail to simultaneously achieve imperceptibility, robustness, and computational efficiency. This work introduces a novel framework for in-generation video watermarking called **SPDMark** (pronounced ‘SpeedMark’) based on **selective parameter displacement** of a video diffusion model. Watermarks are embedded into the generated videos by modifying a subset of parameters in the generative model. To make the problem tractable, the displacement is modeled as an additive composition of layer-wise basis shifts, where the final composition is indexed by the watermarking key. For parameter efficiency, this work specifically leverages low-rank adaptation (LoRA) to implement the basis shifts. During the training phase, the basis shifts and the watermark extractor are jointly learned by minimizing a combination of message recovery, perceptual similarity, and temporal consistency losses. To detect and localize temporal modifications in the watermarked videos, we use a cryptographic hashing function to derive frame-specific watermark messages from the given base watermarking key. During watermark extraction, maximum bipartite matching is applied to recover the correct frame order, even from temporally tampered videos. Evaluations on both text-to-video and image-to-video generation models demonstrate the ability of **SPDMark** to generate imperceptible watermarks that can be recovered with high accuracy and also establish its robustness against a variety of common video modifications.

1 Introduction

The ability of video generation models to generate realistic and temporally coherent videos has improved dramatically within the past 3 years (Blattmann et al., 2023; Wang et al., 2023; OpenAI, 2024; Bao et al., 2024). This raises serious concerns about the provenance of AI-generated videos and the responsible deployment of such generative models. Watermarking has been touted as a practical solution for tracking the provenance of AI-generated content. Recent government regulations such as the EU AI Act (Rijsbosch et al., 2025) and the U.S. Executive Order on AI (Biden, 2023) have also recommended watermarking of AI-generated content to mitigate misuse of such content. An ideal video watermarking must be (i) imperceptible across space and time, (ii) reliably recoverable even after common modifications, and (iii)

computationally efficient. Unlike images, videos introduce the added difficulty of retaining temporal structure: frame drops, swaps, or insertions can break watermark synchronization even when the spatial quality is preserved.

Existing video watermarking approaches fall into two main groups. *Post-hoc* methods (Fernandez et al., 2024) operate on the generated videos but add latency and cannot leverage generative priors. In contrast, in-generation techniques embed the watermark during the video generation process. These schemes can be further categorized into *noise-space* (Hu et al., 2025a) and *model fine-tuning* (Hu et al., 2025b; Jang et al., 2025) methods. Noise-space methods embed the watermarking message within the diffusion noise and decode via DDIM inversion (Song et al., 2020), achieving large message capacity at the cost of high computation. Model fine-tuning methods partially fine-tune the generative model (typically the latent decoder) to embed the watermark message. However, these methods often apply a uniform modulation or embed a single fixed signature, thereby limiting the detection of temporal manipulations. None of the existing video watermarking schemes simultaneously achieve all the desired requirements including imperceptibility, robustness, and computational efficiency.

This work introduces **SPDMark**, a scalable in-generation video watermarking scheme based on the concept of Selective Parameter Displacement (SPD). Instead of perturbing pixels or noise, **SPDMark** embeds watermark messages by selectively displacing parameters of the generative model. The displacement of parameters within the frozen generative model is achieved by activating a sparse combination of learned low-rank basis shifts. A single trained dictionary of low-rank basis shifts supports arbitrary watermark keys without retraining: each key (and each frame) simply selects a different combination of basis shifts. This yields strong imperceptibility and per-frame watermarking at negligible inference overhead. The main contributions of this work can be summarized as follows:

- We propose the Selective Parameter Displacement (**SPDMark**) framework for enabling multi-key in-generation watermarking in video diffusion models.
- To practically realize the **SPDMark** framework, we propose modeling the displacement as an additive composition of layer-wise low-rank basis shifts and determining this composition based on the watermarking key. During training, the dictionary of basis shifts and the watermark extractor are jointly learned by minimizing a combination of message recovery and imperceptibility losses.
- We also propose a mechanism for embedding unique watermark messages in every frame of the generated video and a watermark detection procedure based on maximum bipartite matching and statistical hypothesis testing, which allows for localization of temporal modifications applied to the watermarked video.
- We demonstrate the robustness of **SPDMark** and its ability to preserve video quality through experiments on two video diffusion models and several attack scenarios.

2 Background

2.1 Preliminaries

Notation: Let $\mathcal{G}_\Phi : \mathcal{Z} \times \mathcal{C} \rightarrow \mathcal{X}$ denote a video generation model parameterized by Φ . In general, we assume that the generative model \mathcal{G}_Φ maps a latent noise $\mathbf{z} \in \mathcal{Z}$ and conditioning input $\mathbf{c} \in \mathcal{C}$ (e.g., a text prompt or an image) to a video output $\mathbf{x} \in \mathcal{X}$, i.e., $\mathbf{x} = \mathcal{G}_\Phi(\mathbf{z}, \mathbf{c})$. A video $\mathbf{x} \in \mathcal{X}$ consists of a sequence of T frames $[x_1, x_2, \dots, x_T]$, where x_t represents the t -th frame in the video ($t \in [1, T]$). A watermarking system $\mathcal{W} = (\mathcal{U}_\zeta, \mathcal{V}_\eta)$ consists of an encoder-extractor pair. The *encoder* \mathcal{U}_ζ embeds an M -bit message $\kappa \in \mathcal{K} \subseteq \{0, 1\}^M$ into the generated video, resulting in a watermarked video $\tilde{\mathbf{x}} = \mathcal{U}_\zeta(\kappa) \parallel \mathcal{G}_\Phi(\mathbf{z}, \mathbf{c})$, where \parallel denotes a generic combination of two functions. The watermark *extractor* $\mathcal{V}_\eta : \mathcal{X} \rightarrow \mathcal{K}$ attempts to recover the embedded message $\hat{\kappa} = \mathcal{V}_\eta(\tilde{\mathbf{x}})$ from a watermarked video $\tilde{\mathbf{x}}$.

Problem Statement for Video Watermarking: We consider four participants: (1) The *User* wishes to generate a video conditioned on some input \mathbf{c} , where \mathbf{c} is either a text prompt or an image that controls the semantic content of the generated video. (2) The *Model Owner* has \mathcal{G}_Φ and \mathcal{W} , which enable video generation based on the user’s input \mathbf{c} and distribution of the watermarked video $\tilde{\mathbf{x}}$. (3) The *Verifier* uses \mathcal{V}_η to determine whether the given video contains a valid watermark. (4) The *Adversary* attempts to apply a transformation \mathcal{A} to a video, either to remove the watermark from a valid watermarked video $\tilde{\mathbf{x}}$ or to forge a valid watermark into a non-watermarked video \mathbf{x} (which could be natural or synthetically generated). We assume that the adversary has no access to Φ , ζ , or η , and that \mathcal{A} is bounded (mostly preserving the visual content).

An ideal watermarking scheme should satisfy the following four requirements: (i) **Imperceptibility:** \tilde{x} should be perceptually indistinguishable from x (for any \mathbf{c}) under visual inspection by the user. (ii) **Message Recoverability:** Message $\hat{\kappa}$ extracted from valid watermarked videos should match the embedded message κ with high probability, and the false positive rate (probability of recovering κ from non-watermarked videos) should be low. (iii) **Robustness:** The watermark should be resistant against small modifications \mathcal{A} (e.g., compression, cropping, frame drop, etc.) applied by the adversary. (iv) **Computational Efficiency:** The computational effort required to embed and extract the watermark must be small compared to video generation (ideally, offline training effort should also be minimal).

2.2 Image and Video Diffusion Models

Diffusion models (Ho et al., 2020; Dhariwal and Nichol, 2021) synthesize data by learning to reverse a gradual noising process. Latent Diffusion Models (LDMs) (Rombach et al., 2022) for images improve efficiency by operating in a compressed latent space: an encoder \mathcal{E} maps an image to a latent code, a denoiser (UNet (Ronneberger et al., 2015) or Diffusion Transformer (Peebles and Xie, 2023)) iteratively refines the noised latent code, and a decoder \mathcal{D} reconstructs the output image. The encoder-decoder pair can be considered as a Variational Auto-Encoder (VAE). Video diffusion models extend this pipeline to capture spatiotemporal structure. Early systems such as ModelScope (Wang et al., 2023) and Stable Video Diffusion (Blattmann et al., 2023) pair 2D VAEs with 3D UNets, while recent models including Sora (OpenAI, 2024) and Vidu (Bao et al., 2024) adopt 3D VAEs and DiT backbones to model long-range motion. These architectural differences impact our watermarking system design: schemes that target the noising process or the denoiser may not transfer across UNet- and DiT-based models, and the set of parameters selected for displacement (encoder, denoiser, or decoder) affects the robustness and verification cost. SPDMark therefore embeds watermarks in the decoder \mathcal{D} , an architecture-agnostic component shared by both UNet- and Transformer-based video diffusion models.

2.3 Watermarking for Image Generation Models

Watermarking for generative models generally follows two paradigms: post-hoc and in-generation. Post-hoc methods (Saha et al., 2020) embed signals after generation using encoder-decoder networks, achieving good imperceptibility but adding latency and remaining decoupled from the generative model. In-generation methods embed watermarks directly in the diffusion process. Noise-space techniques such as Tree-Ring (Wen et al., 2023) and Gaussian Shading (Yang et al., 2024), modify the initial noise and decode via DDIM inversion (Song et al., 2020); however, inversion is computationally expensive and fragile under perturbations. Model fine-tuning approaches avoid inversion by modifying model weights: Stable Signature (Fernandez et al., 2023) and WOUAF (Kim et al., 2024) fine-tune diffusion decoders, and AQuaLoRA (Feng et al., 2024) uses LoRA modules for image-level embedding. While these methods offer strong imperceptibility, they lack temporal coherence required for video generation.

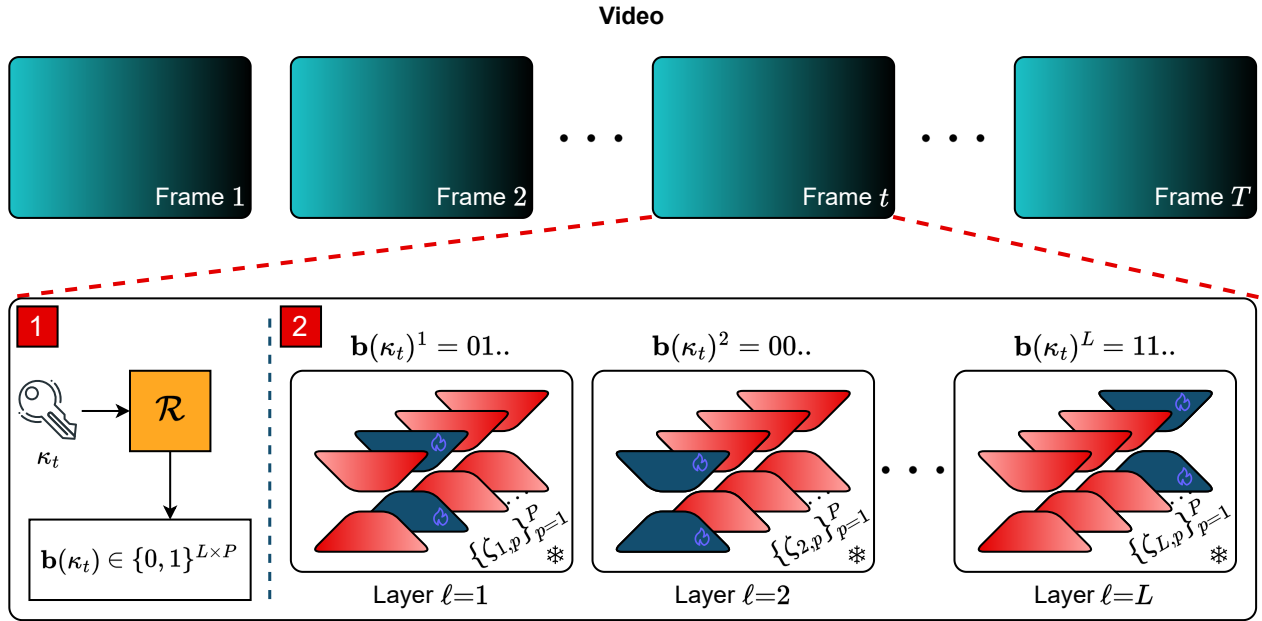


Figure 1: SPDMark pipeline. Watermarking key κ is expanded into per-frame messages $\{\kappa_t\}$. Each κ_t is mapped to a binary mask $\mathbf{b}(\kappa_t)$, yielding the parameter displacement $\Delta\Phi_M(\kappa_t) = \mathbf{b}(\kappa_t) \otimes \zeta$, which is applied to the frozen decoder to produce the watermarked video $\tilde{\mathbf{x}}$. The watermark extractor \mathcal{V}_η recovers the messages frame-wise; verification uses graph-based alignment and hypothesis testing (Sec. 3.2).

2.4 Video Watermarking

Since video watermarking requires preserving both spatial imperceptibility and temporal coherence, extensions of image watermarking approaches have been proposed for videos.

Noise-space methods: VideoShield (Hu et al., 2025a) perturbs the initial diffusion noise and decodes messages via DDIM inversion, enabling tamper localization but incurring high computational cost and failing under frame reordering. VideoMark (Hu et al., 2025b) adds per-frame pseudo-random noise with error-correcting codes to improve matching, but still inherits the fragility and overhead of full inversion.

Model fine-tuning methods: LVMark (Jang et al., 2025) jointly trains a modified latent decoder and 3D extractor, achieving strong robustness but modulating all layers uniformly, which limits per-frame control and harms visual quality. VideoSignature (VidSig) (Huang et al., 2025) freezes perceptually sensitive layers (PAS) and adds a temporal alignment module, but embeds a single fixed signature rather than frame-specific messages.

Post-hoc methods: VideoSeal (Fernandez et al., 2024) embeds watermarks after generation using a lightweight U-Net and ViT extractor, aided by differentiable augmentations and codec simulation. While effective for compression, its post-generation nature adds latency and cannot leverage generative priors. SPDMark differs from the above methods by learning a fixed dictionary of low-rank basis shifts that can be dynamically composed per frame according to arbitrary binary messages, enabling efficient multi-key watermarking with per-frame control and no retraining. SPDMark is also computationally efficient because it avoids inversion entirely.

3 Proposed Method: SPDMark

SPDMark is an in-generation video watermarking method, where the core idea is to embed the watermark by selectively modifying the parameters of the given video diffusion model and jointly learn a lightweight

watermark extractor.

3.1 Selective Parameter Displacement Framework

Let \mathcal{G}_Φ be the given video generation model and κ be the given watermarking key. Let \mathbf{c} be any conditioning input provided by the user and \mathbf{z} be any latent noise chosen by the model owner. The objective of the parameter displacement framework is to displace the parameters Φ of \mathcal{G} such that the videos generated by the displaced model embed the watermark key κ . Let $(\Phi + \Delta\Phi)$ be the parameters of the displaced model, where $\Delta\Phi$ denotes the displacement. Since $\Delta\Phi$ encodes the key κ , the mapping from κ to $\Delta\Phi$ can be considered as the watermarker encoder. The challenge is to learn this encoder carefully so that the applied displacement does not affect the visual quality of the watermarked videos. Therefore, we need to design the watermarking system \mathcal{W} and learn the displacement such that:

$$\min_{\zeta, \eta} \mathcal{L}_{\text{imp}}(\mathbf{x}, \tilde{\mathbf{x}}) + \mathcal{L}_{\text{rec}}(\mathcal{V}_\eta(\tilde{\mathbf{x}}), \kappa), \quad (1)$$

where $\tilde{\mathbf{x}} = \mathcal{G}_{\Phi + \Delta\Phi}(\mathbf{z}, \mathbf{c})$ and $\Delta\Phi = \mathcal{U}_\zeta(\kappa)$. In the above formulation, \mathcal{L}_{imp} and \mathcal{L}_{rec} are loss functions that enforce the imperceptibility and message recoverability requirements, respectively.

To make the problem of learning the parameter displacement $\Delta\Phi$ tractable, we first partition the parameters of the given generative model into two components Φ_U and Φ_M , where Φ_U denotes the parameters that remain untouched and Φ_M denotes the parameters to be modified. Correspondingly, the displacement $\Delta\Phi$ is also split into two components, where the first component is zero and the second component $\Delta\Phi_M$ needs to be learned.

$$\Phi = \begin{bmatrix} \Phi_U \\ \Phi_M \end{bmatrix}, \Delta\Phi = \begin{bmatrix} \mathbf{0} \\ \Delta\Phi_M \end{bmatrix}. \quad (2)$$

Next, we assume that the parameters to be modified (Φ_M) are spread across L distinct layers in the generative model. Let ϕ_ℓ denote the parameters of layer ℓ , $\ell \in [1, L]$ and $\Delta\phi_\ell$ denote the corresponding displacement. Hence,

$$\Phi_M = \begin{bmatrix} \phi_1 \\ \phi_2 \\ \vdots \\ \phi_L \end{bmatrix}, \Delta\Phi_M = \begin{bmatrix} \Delta\phi_1 \\ \Delta\phi_2 \\ \vdots \\ \Delta\phi_L \end{bmatrix}. \quad (3)$$

In each layer $\ell \in [1, L]$, the displacement $\Delta\phi_\ell$ is further modeled as an **additive composition of P basis shifts**. Let $\{\zeta_{\ell,p}\}_{p=1}^P$ denote the set of basis shifts in layer ℓ . Therefore,

$$\Delta\phi_\ell = \sum_{p=1}^P b_{\ell,p} \zeta_{\ell,p}, \quad (4)$$

where $b_{\ell,p} \in \{0, 1\}$ is a binary mask indicating if the corresponding basis shift is selected. Let $\zeta = \{\{\zeta_{\ell,p}\}_{p=1}^P\}_{\ell=1}^L$ denote the set of all basis shifts across all layers and $\mathbf{b} = \{\{b_{\ell,p}\}_{p=1}^P\}_{\ell=1}^L \in \{0, 1\}^{L \times P}$ be the set of all mask values. Since our goal is to define the displacement $\Delta\Phi$ as a function of the watermark key κ , we employ a key mapping procedure to determine the binary mask using κ . Let $\mathbf{b}(\kappa)$ be the binary mask indexed by κ . Thus,

$$\Delta\Phi_M = \mathbf{b}(\kappa) \otimes \zeta = \begin{bmatrix} \sum_{p=1}^P b_{1,p} \zeta_{1,p} \\ \sum_{p=1}^P b_{2,p} \zeta_{2,p} \\ \vdots \\ \sum_{p=1}^P b_{L,p} \zeta_{L,p} \end{bmatrix}. \quad (5)$$

Equations (1) through (5) together define the proposed Selective Parameter Displacement framework for video watermarking (SPDMark).

3.2 Practical Implementation of SPDMark

To realize the SPDMark framework in practice, we make the following implementation choices.

Key Mapping: Though there are many ways to map the watermark key κ to the binary mask \mathbf{b} , we use the following simple procedure. Initially, we set all the binary masks $b_{\ell,p}$ to zero ($\forall \ell \in [1, L], p \in [1, P]$). We assume that the key length is $M = L \log_2 P$ bits. Then, we partition the key κ into L chunks of $\log_2 P$ bits, i.e., $\kappa = [\kappa_1, \kappa_2, \dots, \kappa_L]$, where each κ_ℓ contains $\log_2 P$ bits. Let $i_\ell = \text{bin2dec}(\kappa_\ell)$ be the decimal representation of κ_ℓ . Note that $i_\ell \in [0, P - 1]$. We set $b_{\ell, i_\ell + 1}$ to value 1 in each layer ℓ . Thus, the key κ gets mapped to the binary mask \mathbf{b} and consequently, the displacement $\Delta\Phi$ becomes a function of κ .

$$\Delta\Phi_M(\kappa) = \mathbf{b}(\kappa) \otimes \zeta = \begin{bmatrix} \zeta_{1, i_1 + 1} \\ \zeta_{2, i_2 + 1} \\ \vdots \\ \zeta_{L, i_L + 1} \end{bmatrix}, \quad (6)$$

where $i_\ell = \text{bin2dec}(\kappa_\ell)$. Note that the above key mapping procedure selects only a single basis shift in each layer ℓ for parameter displacement.

Layer Selection: This work assumes that the video generation model is a latent diffusion model, consisting of an encoder, a denoiser, and a decoder, as explained in Section 2.2. To preserve the quality of video generation, we leave the parameters of the encoder and denoiser untouched and apply SPD only to the diffusion model decoder.

Choice of basis shifts: While it is possible to learn the basis shifts ζ directly, such an approach is not parameter efficient. Hence, we borrow the idea of low-rank adaptation (LoRA) (Hu et al., 2022) and instantiate the basis shifts using low-rank matrix decompositions. Each basis shift $\zeta_{\ell,p}$ is modeled as a low-rank update to the layer parameters as follows.

$$\begin{aligned} \zeta_{\ell,p} &= A_{\ell,p} B_{\ell,p}, \\ A_{\ell,p} &\in \mathbb{R}^{d \times r}, \quad B_{\ell,p} \in \mathbb{R}^{r \times d}, \quad r \ll d. \end{aligned} \quad (7)$$

Let $\mathbf{h}_{\ell-1}$ be the input to layer ℓ in the original diffusion model and let $\mathbf{h}_\ell = \mathcal{F}_{\phi_\ell}(\mathbf{h}_{\ell-1})$ be its output. After parameter displacement, the output of layer ℓ is computed as:

$$\mathbf{h}_\ell = \mathcal{F}_{\phi_\ell}(\mathbf{h}_{\ell-1}) + \alpha \mathcal{F}_{\Delta\phi_\ell}(\mathbf{h}_{\ell-1}), \quad (8)$$

where $\Delta\phi_\ell = \zeta_{\ell, p^*} = A_{\ell, p^*} B_{\ell, p^*}$, $p^* = (i_\ell + 1)$ denotes the basis shift for layer ℓ selected based on κ , and α is a fixed scalar.

Per-Frame Watermark Message Generation: To detect and localize temporal modifications in the watermarked video, it is essential to embed unique watermark messages in each frame of the video. For a T -frame video, we derive frame-specific watermark messages using a secret key K_{base} and a time-varying message as inputs to a cryptographic hash function \mathcal{H} (e.g., HMAC-SHA256):

$$\kappa_t = \text{Trunc}_M(\mathcal{H}(K_{\text{base}}, [\kappa \ t])), \quad t = 1, \dots, T. \quad (9)$$

where $[\kappa \ t]$ denotes the time-varying message obtained by concatenating κ with t and Trunc_M denotes that the resulting hash value is truncated to the first M bits. Consequently, the parameter displacement is also

frame-specific.

Watermark Extractor: Since the embedded watermark message is frame-specific, the watermark extractor \mathcal{V}_η is designed to operate on individual frames of the video. Specifically, we employ a ResNet-50 (He et al., 2016) model pretrained on ImageNet (Deng et al., 2009) and replace the final fully connected layer with a linear head that outputs M logits per frame.

Loss Functions: To enforce the message recoverability requirement, we employ the binary cross entropy with logits loss ($\text{BCE}_{\text{logits}}$). Specifically, for a watermarked video $\tilde{\mathbf{x}}$,

$$\mathcal{L}_{\text{rec}}(\mathcal{V}_\eta(\tilde{\mathbf{x}}), \kappa) = \mathbb{E}_{t \sim T} [\text{BCE}_{\text{logits}}(\mathcal{V}_\eta(\tilde{x}_t), \kappa_t)], \quad (10)$$

where \tilde{x}_t is the t -th frame in $\tilde{\mathbf{x}}$ and κ_t is the frame-specific watermark message.

To enforce the imperceptibility constraint, we use a weighted combination of perceptual similarity (defined based on LPIPS (Zhang et al., 2018)) and temporal consistency losses. While the perceptual similarity (PS) loss encourages the watermarked video to stay closer to the corresponding original video without watermark, the temporal consistency (TC) loss ensures smooth transition between successive frames of the video (thereby avoiding the flickering effect). Let $\mathbf{x} = \mathcal{G}_\Phi(\mathbf{z}, \mathbf{c})$ be the non-watermarked video generated by the original model and $\tilde{\mathbf{x}} = \mathcal{G}_{\Phi+\Delta\Phi}(\mathbf{z}, \mathbf{c})$ be the watermarked video generated by the displaced model with the same \mathbf{z} and \mathbf{c} . The imperceptibility loss is defined as:

$$\begin{aligned} \mathcal{L}_{\text{imp}}(\mathbf{x}, \tilde{\mathbf{x}}) &= \lambda_{ps} \mathbb{E}_{t \sim T} [\text{LPIPS}(x_t, \tilde{x}_t)] \\ &+ \lambda_{tc} \mathbb{E}_{t \sim T} [\|\delta y_t - \delta \tilde{y}_t\|_1], \end{aligned} \quad (11)$$

where $y = (0.299 x^{(R)} + 0.587 x^{(G)} + 0.114 x^{(B)})$ represents the luminance of an image whose RGB channels are denoted as $x^{(R)}$, $x^{(G)}$, and $x^{(B)}$, respectively. Furthermore, $\delta y_t = (y_t - y_{t-1})$ and $\delta \tilde{y}_t = (\tilde{y}_t - \tilde{y}_{t-1})$ denote the luminance differences between successive frames in the non-watermarked and watermarked videos, respectively. Here, λ_{ps} and λ_{tc} are the weights assigned to the PS and TC losses, respectively. For the TC loss, the expectation is computed over $(T - 1)$ frame differences. Since the watermarking procedure must be agnostic to the watermark key κ , input condition \mathbf{c} , and latent noise \mathbf{z} , the optimization in Eq. 1 (based on losses defined in Eqs. 10 and 11) is performed in expectation over $\kappa \sim \mathcal{K}$, $\mathbf{c} \sim \mathcal{C}$, and $\mathbf{z} \sim \mathcal{Z}$.

Verification of Watermark Validity: During verification, the verifier applies the watermark extractor \mathcal{V}_η to the individual frames in the given video \mathbf{x}^* to recover a sequence of watermark messages $\hat{\mathbf{K}} = [\hat{\kappa}_1, \hat{\kappa}_2, \dots, \hat{\kappa}_{T_r}]$, where T_r is the number of frames in the given video. To verify whether \mathbf{x}^* contains a valid watermark, the verifier needs access to the watermark message κ used by the model owner for generating the watermarked video. Given κ and number of frames T in the watermarked video, it is straightforward to generate the frame-specific messages $\mathbf{K} = [\kappa_1, \kappa_2, \dots, \kappa_T]$ used by the model owner using Eq. 9. Note that due to temporal modifications (e.g., frame drops, insertions, reordering, etc.) T_r may not be equal to T and there may be temporal misalignment between the frames. We pose the problem of finding matching frames as a *maximum bipartite graph matching* problem and solve it using the Hungarian algorithm (Kuhn, 1955). Specifically, the set of messages in \mathbf{K} and $\hat{\mathbf{K}}$ are modeled as a bipartite graph with the edge weights between vertices in \mathbf{K} and $\hat{\mathbf{K}}$ defined as:

$$\bar{S}_{m,n} = 1 - \frac{\psi(\kappa_m, \hat{\kappa}_n)}{M}, \quad (12)$$

where ψ is the Hamming distance between two binary strings of length M , $m \in [1, T]$, and $n \in [1, T_r]$. Note that the edge weights $\bar{S}_{m,n}$ represent the similarity (proportion of matched bits) between messages κ_m and $\hat{\kappa}_n$. We compute one-to-one assignment (alignment) between the two sets of messages maximizing

Table 1: Video quality and watermark detection performance of SPDMark compared to existing video watermarking methods. All values are averaged across test videos. \uparrow indicates higher is better. The best result in each column is shown in **bold** and the second is underlined.

| Model | Method | Extraction | | Video Quality | | | |
|------------------------|-----------------------|----------------|--------------------|---------------|---------------|---------------|---------------|
| | | Bit Len. | Bit Acc \uparrow | SC \uparrow | BC \uparrow | MS \uparrow | IQ \uparrow |
| SVD-XT | VideoShield | 512 | 0.979 | 0.954 | <u>0.954</u> | 0.956 | 0.695 |
| | VideoSeal | 256 | 0.999 | <u>0.955</u> | 0.950 | <u>0.961</u> | 0.682 |
| | VidSig | 48 | 0.958 | 0.951 | 0.953 | 0.956 | <u>0.693</u> |
| | SPDMark (Ours) | 28×25 | <u>0.995</u> | 0.966 | 0.958 | 0.975 | 0.690 |
| ModelScope (MS) | VideoShield | 512 | 1.000 | 0.927 | 0.954 | <u>0.963</u> | <u>0.612</u> |
| | VideoSeal | 256 | 0.999 | 0.944 | 0.965 | 0.964 | 0.614 |
| | VidSig | 48 | 1.000 | <u>0.932</u> | <u>0.955</u> | <u>0.963</u> | 0.610 |
| | SPDMark (Ours) | 28×16 | 0.988 | 0.900 | 0.937 | 0.960 | 0.555 |

the total similarity.

$$(\pi^*, \rho^*) = \arg \max_{\pi, \rho} \sum_i \bar{S}_{\pi_i, \rho_i}. \quad (13)$$

Let $\mathcal{M} = \{(\pi_i, \rho_i)\}_{i=1}^{|\mathcal{M}|}$ denote the set of assignments made by the Hungarian algorithm, where $|\mathcal{M}|$ is the number of assignments. To verify the validity of each frame assignment, we perform the following hypothesis test. Let $S_{m,n} = (M - \psi(\kappa_m, \hat{\kappa}_n))$ denote the number of matched bits between κ_m and $\hat{\kappa}_n$. Under the null hypothesis H_0 (no valid watermark present), the number of matched bits S follows a Binomial distribution, i.e., $S \sim \text{Binomial}(M, \frac{1}{2})$ because bit matches are expected to be random in this case. For a target frame-level false positive rate γ_f , we compute:

$$\tau_f = \min \{ \tau : \Pr(S \geq \tau | H_0) \leq \gamma_f \}. \quad (14)$$

A frame-level assignment is considered valid only if $S_{\pi_i, \rho_i} \geq \tau_f$. Let $\mathcal{Q} = \{(\pi_i, \rho_i) | S_{\pi_i, \rho_i} \geq \tau_f\}_{i=1}^{|\mathcal{Q}|} \subseteq \mathcal{M}$ be the set of valid assignments, where $|\mathcal{Q}|$ is the number of valid assignments. Let $p_f = \Pr(S \geq \tau_f | H_0)$. Under H_0 , the number of valid assignments also follows a Binomial distribution, i.e., $|\mathcal{Q}| \sim \text{Binomial}(|\mathcal{M}|, p_f)$. For a target video-level false positive rate γ_v , we compute:

$$\tau_v = \min \{ \tau : \Pr(|\mathcal{Q}| \geq \tau | H_0) \leq \gamma_v \}. \quad (15)$$

The given video \mathbf{x}^* is deemed to contain a valid watermark only if $|\mathcal{Q}| \geq \tau_v$. Finally, it must be noted that the set of valid assignments \mathcal{Q} provides the information necessary to localize temporal modifications in a watermarked video.

4 Experiments

4.1 Implementation Details

Base Models. We implement SPDMark on two video diffusion architectures: *Stable Video Diffusion (SVD-XT)* (Blattmann et al., 2023): an image-to-video model configured for 576×1024 resolution with 25 frames at 7 fps and 25 inference steps; *ModelScope (MS)* (Wang et al., 2023): a text-to-video model operating at 256×256 resolution with 16 frames and 50 denoising steps. For MS, we evaluate on 50 prompts from the Vbench test split (Huang et al., 2024) covering five categories (Animal, Human, Plant, Scenery, Vehicles; 10 each), generating 4 videos per prompt ($50 \times 4 = 200$ videos). For SVD-XT, we first synthesize 200

conditioning images with a T2I model (LDM v1.5 (Rombach et al., 2022)) using the same 50 prompts, then feed these images to SVD-XT to obtain a matched set of 200 i2v videos. We train on 10,000 videos from OpenVid-1M (Nan et al., 2024), additional training details are provided in the Appendix.

Basis-selection configuration. We attach learned basis shifts to the latent decoder’s $L=14$ spatial ResNet blocks. Each block has $P=4$ parallel low-rank adapters (rank $r=32$), giving $\log_2 P=2$ bits per block and a payload of 28 bits per frame.

Extractor \mathcal{V}_η . We use a frame-wise ResNet-50 (He et al., 2016) (ImageNet-pretrained (Deng et al., 2009)) with the final FC replaced by a linear head outputting 28 logits per frame. Given $v \in \mathbb{R}^{B \times T \times 3 \times H \times W}$, frames are normalized to ImageNet statistics and processed independently to yield $[B, T, 28]$ logits. Training minimizes equation 10 against κ_t . At inference, we use test-time batch normalization, computing BN statistics over all T frames of each test video to stabilize predictions under the length/resolution mismatch. Additional details on computational cost and efficiency are provided in Appendix.

4.2 Evaluation Metrics

We evaluate SPDMark along three axes: imperceptibility, message recoverability, and temporal and spatial robustness

Generation Quality. We report VBench (Huang et al., 2024) metrics: Subject Consistency (SC), Background Consistency (BC), Motion Smoothness (MS), and Imaging Quality (IQ) using the released evaluator. Additional details about these metrics are in the Appendix.

Watermark Extraction. Given the valid aligned pairs $\mathcal{Q} = \{(\pi_i, \rho_i)\}$, we compute

$$\begin{aligned} \text{Bit Acc} &= \frac{1}{|\mathcal{Q}|} \sum_{(\pi, \rho) \in \mathcal{Q}} \frac{S_{\pi, \rho}}{M}, \\ \text{Order Acc} &= \frac{1}{|\mathcal{Q}| - 1} \sum_i \mathbb{I}[\rho_i < \rho_{i+1}]. \end{aligned} \tag{16}$$

For temporal attacks, we additionally report precision, recall, and F1 over modified frame indices.

4.3 Robustness and Attack Protocol

To evaluate robustness under realistic video degradation, we test SPDMark across three categories of attacks: (i) photometric and spatial distortions (Gaussian noise, blur, geometric transforms, compression artifacts), (ii) temporal manipulations (frame drops, swaps, inserts, trims), and (iii) real-world post-processing such as video recompression and screen-recording-style degradation. These attacks capture common transformations introduced during sharing, editing, or platform transcoding. Full attack definitions, parameter settings, and implementation details are provided in the Appendix.

4.4 Results

Watermark Extraction and Generation Quality. We compare SPDMark against VideoShield, VideoSeal, and VidSig. Table 1 reports extraction accuracy and video quality metrics. On SVD-XT, SPDMark achieves a bit accuracy of 99.5%, comparable to the strongest baselines, and maintains stable performance on ModelScope (98.8%) despite its lower spatial resolution. Across video quality metrics, SPDMark performs competitively: it achieves the highest subject consistency (SC) and motion smoothness (MS) on SVD-XT, indicating that the learned routing patterns do not disrupt the underlying temporal structure. Background consistency (BC) and image quality (IQ) are slightly lower than those of VideoSeal and VideoShield, reflecting the trade-off introduced by modulating decoder parameters directly rather than applying a post-processing watermark network. Overall, SPDMark preserves semantic content and scene layout while introducing mild texture



Figure 2: Visual comparison across watermarking methods on SVD-XT (first row) and ModelScope (second row). For each method, we show non-consecutive frames (0 and 2).

Table 2: Robustness of SPDMark under photometric, temporal, and real-world post-processing attacks. Metrics report average watermark Bit Acc (\uparrow). The best average robust result is shown in **bold** and the second best is underlined.

| <i>SVD-XT</i> | | | | | | | | | |
|--|------------|----------|-------------|----------------|--------------|-------------|---------------|----------------|--------------|
| (I: Photometric and Spatial Attacks, II: Temporal Tampering, III: Post-Processing) | | | | | | | | | |
| Method (\downarrow)/ Attack (\rightarrow) | I. Gauss | I. Blur | I. Crop | I. Rotate | I. Rescale | I. ColorJit | II. Drop | II. Swap | |
| VideoShield | 0.964 | 0.962 | 0.521 | 0.507 | 0.976 | 0.978 | – | 0.935 | – |
| VideoSeal | 0.972 | 0.998 | 0.996 | 0.687 | 0.999 | 0.999 | 0.999 | 0.999 | – |
| VidSig | 0.937 | 0.420 | 0.438 | 0.521 | 0.688 | 0.958 | 0.958 | 0.958 | – |
| SPDMark (Ours) | 0.958 | 0.847 | 0.989 | 0.930 | 0.910 | 0.993 | 0.988 | 0.994 | – |
| Method/Attack | II. Insert | II. Trim | III. Recomp | III. ScreenRec | III. Denoise | III. STTN | III. Subtitle | III. Crop&Drop | Avg. |
| VideoShield | – | – | 0.906 | 0.653 | 0.961 | 0.991 | 0.973 | 0.501 | 0.833 |
| VideoSeal | 0.999 | 0.998 | 0.838 | 0.598 | 0.999 | 0.999 | 0.999 | 0.513 | <u>0.912</u> |
| VidSig | 0.958 | 0.937 | 0.521 | 0.563 | 0.438 | 0.708 | 0.500 | 0.458 | 0.685 |
| SPDMark (Ours) | 0.994 | 0.993 | 0.880 | 0.837 | 0.921 | 0.878 | 0.993 | 0.856 | 0.935 |

| <i>ModelScope (MS)</i> | | | | | | | | | |
|--|------------|----------|-------------|----------------|--------------|-------------|---------------|----------------|--------------|
| (I: Photometric and Spatial Attacks, II: Temporal Tampering, III: Post-Processing) | | | | | | | | | |
| Method/Attack | I. Gauss | I. Blur | I. Crop | I. Rotate | I. Rescale | I. ColorJit | II. Drop | II. Swap | |
| VideoShield | 1.000 | 0.999 | 0.651 | 0.523 | 1.000 | 1.000 | – | 0.997 | – |
| VideoSeal | 0.913 | 0.951 | 0.998 | 0.972 | 0.976 | 0.999 | 0.990 | 0.999 | – |
| VidSig | 0.937 | 0.542 | 0.958 | 0.771 | 0.563 | 0.979 | 1.000 | 1.000 | – |
| SPDMark (Ours) | 0.985 | 0.972 | 0.963 | 0.979 | 0.988 | 0.988 | 0.980 | 0.988 | – |
| Method/Attack | II. Insert | II. Trim | III. Recomp | III. ScreenRec | III. Denoise | III. STTN | III. Subtitle | III. Crop&Drop | Avg. |
| VideoShield | – | – | 0.998 | 0.853 | 1.000 | 1.000 | 1.000 | 0.500 | 0.886 |
| VideoSeal | 0.999 | 0.998 | 0.531 | 0.511 | 0.999 | 0.999 | 0.982 | 0.674 | <u>0.906</u> |
| VidSig | 1.000 | 1.000 | 0.521 | 0.400 | 0.688 | 0.979 | 1.000 | 0.646 | 0.812 |
| SPDMark (Ours) | 0.987 | 0.983 | 0.794 | 0.766 | 0.984 | 0.988 | 0.979 | 0.784 | 0.944 |

changes (Fig. 2). Additional qualitative examples and extended comparisons are provided in the Appendix. VBench metrics indicate that SPDMark maintains competitive video quality despite directly modulating decoder parameters. On SVD-XT, it achieves the highest motion smoothness ($MS = 0.975$), suggesting that the routing-based watermark does not disrupt global temporal structure. Subject and background consistency ($SC/BC = 0.966/0.958$) are also comparable to or slightly above those of existing in-generation methods. Image quality (IQ) shows moderate degradation relative to post-processing approaches such as VideoSeal, reflecting the trade-off introduced by embedding the watermark within the generative process rather than applying an external refinement network. Nonetheless, qualitative results (Fig. 2) show that semantic content and scene layout remain intact, with changes primarily limited to mild texture variations.

Watermark Robustness. Table 2 summarizes robustness across 16 photometric, geometric, temporal, and post-processing attacks. On average, SPDMark achieves 93.5% robustness on SVD-XT and 94.4% on ModelScope, outperforming VideoShield, VidSig, and VideoSeal. Across most photometric distortions (Gaussian noise, color jitter, rescaling), SPDMark maintains high accuracy, often above 95%. Performance under strong blur is lower than VideoSeal, consistent with the fact that post-processing methods can

optimize directly for frequency-domain resilience, whereas **SPDMark** embeds its signal within the generative process. Under geometric changes such as rotation and cropping, **SPDMark** performs substantially better than noise-space approaches like VideoShield, reflecting improved spatial stability. For frame-level manipulations (drops, swaps, insertions, and trims), **SPDMark** achieves high extraction rates, aided by the per-frame alignment verification. Under recompression, denoising, and screen recording, **SPDMark** retains robustness that is competitive with or higher than other in-generation methods. While VideoSeal occasionally performs better under certain compression settings, **SPDMark** still maintains strong average performance. Overall, the results suggest that it yields robustness across a diverse range of perturbations, with particular strength in geometric and temporal settings.

Table 3: Performance under temporal attacks. Frame Drop/Insert are evaluated with Precision, Recall, and F1 (\uparrow), while Swap attacks use Order Accuracy (\uparrow).

| Attack | SVD-XT | ModelScope (MS) |
|--|-----------------------|-----------------------|
| <i>Frame-altering Attacks (Prec./Rec./F1)</i> | | |
| Frame Drop | 0.999 / 0.999 / 0.999 | 0.998 / 0.999 / 0.999 |
| Frame Insert | 0.996 / 0.994 / 0.995 | 0.998 / 0.999 / 0.999 |
| <i>Order-altering Attacks (Order Accuracy)</i> | | |
| Random Swap | 1.000 | 1.000 |
| Adjacent Swap | 1.000 | 1.000 |

4.5 Ablation Studies

4.5.1 Basis-Selection Placement and Bit Capacity

We study how the placement and number of basis shift sites affect per-frame capacity and fidelity. In our decoder, L spatial ResNet blocks and one attention block (Q/K/V) are potential sites. We compare three placements (all with $P=4$): **G1** uses one site per ResNet block (shared conv1/conv2), $L=14 \Rightarrow M=28$ bits/frame; **G2** adds the three attention projections, $L=17 \Rightarrow M=34$; **G3** treats conv1 and conv2 as separate sites, $L=28 \Rightarrow M=56$. Figure 3 shows results for the three configurations. As capacity increases from 28 bits (G1) to 56 bits (G3), we observe lower bit accuracy (99.5% \rightarrow 70.5%) and robustness (93.5% \rightarrow 70.2%), while quality metrics show minimal variation. Based on these results, we use a key of bit length (28 bits) for all other experiments.

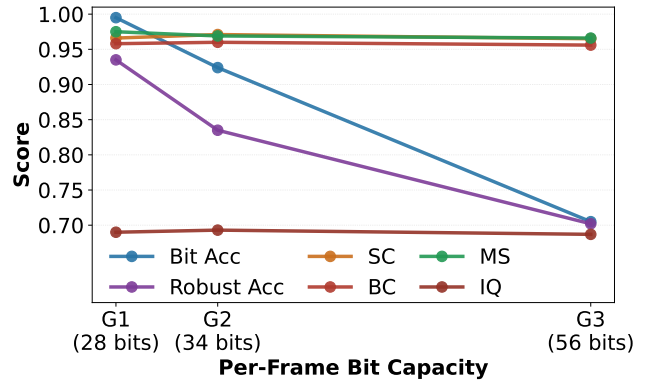


Figure 3: Bit Acc, Robust Acc, SC, BC, MS, and IQ vs. per-frame bit length.

Sampling configurations. Table 4 reports an ablation on SVD-XT covering the number of generated frames, diffusion steps, and classifier-free guidance scale. Across all settings, **SPDMark** maintains high extraction reliability, with bit accuracy remaining above 94% for short clips (8 frames) and reaching 99% or higher for 16–32 frames. Robust accuracy shows a modest improvement with longer videos (from 0.880 at 8 frames to 0.933 at 32 frames), which is expected since additional frames provide more opportunities for correct alignment in the verification stage. Varying the number of diffusion steps (10 vs. 50) and guidance strength (1 vs. 5) has limited influence on watermark recovery or video-quality metrics, indicating that the

Table 4: Sampling and ablation studies on **SVD-XT**. Robust means bit accuracy under the attack suite used in Table 2

| Factor | Setting | Bit Acc (\uparrow) | Robust | SC (\uparrow) | BC (\uparrow) | MS (\uparrow) | IQ (\uparrow) |
|----------|---------|------------------------|--------------|-------------------|-------------------|-------------------|-------------------|
| Frames | 8 | 0.942 | 0.880 | <u>0.976</u> | 0.968 | <u>0.970</u> | 0.721 |
| | 16 | <u>0.989</u> | <u>0.913</u> | 0.978 | 0.962 | 0.972 | <u>0.710</u> |
| | 32 | 0.996 | 0.933 | 0.965 | 0.959 | 0.961 | 0.700 |
| Steps | 10 | 0.989 | 0.902 | 0.951 | 0.948 | 0.970 | 0.630 |
| | 50 | 0.995 | 0.911 | 0.971 | 0.958 | 0.968 | 0.713 |
| Guidance | 1 | 0.998 | 0.915 | 0.923 | 0.940 | 0.962 | 0.640 |
| | 5 | 0.991 | 0.910 | 0.971 | 0.960 | 0.967 | 0.719 |

basis-shift perturbations applied in the decoder interact weakly with the sampling procedure. Additional results for ModelScope are provided in the Appendix.

5 Conclusion

We presented **SPDMark**, an in-generation video watermarking framework based on Selective Parameter Displacement. By modeling watermarks as key-conditioned combination of learned low-rank basis shifts, **SPDMark** enables efficient multi-key embedding without per-key retraining. Our approach addresses key limitations of existing methods: it avoids the computational burden and fragility of DDIM inversion, provides per-frame key control, and integrates watermarking directly within the generative process. It enables robust extraction and forensic analysis. **SPDMark** demonstrates that carefully designed parameter displacement provides an effective and practical watermarking mechanism for modern video diffusion models, offering a compelling balance between detection accuracy, temporal coherence, and computational efficiency. Several directions could extend this work such as adaptive displacement that concentrates watermarks in perceptually less sensitive regions based on content analysis, and extension to other generative modalities.

References

- Fan Bao, Chendong Xiang, Gang Yue, Guande He, Hongzhou Zhu, Kaiwen Zheng, Min Zhao, Shilong Liu, Yaole Wang, and Jun Zhu. Vidu: a highly consistent, dynamic and skilled text-to-video generator with diffusion models. arXiv preprint arXiv:2405.04233, 2024.
- Joseph R Biden. Executive order on the safe, secure, and trustworthy development and use of artificial intelligence. 2023.
- Andreas Blattmann, Tim Dockhorn, Sumith Kulal, Daniel Mendelevitch, Maciej Kilian, Dominik Lorenz, Yam Levi, Zion English, Vikram Voleti, Adam Letts, et al. Stable video diffusion: Scaling latent video diffusion models to large datasets. arXiv preprint arXiv:2311.15127, 2023.
- Mathilde Caron, Hugo Touvron, Ishan Misra, Hervé Jégou, Julien Mairal, Piotr Bojanowski, and Armand Joulin. Emerging properties in self-supervised vision transformers, 2021. URL <https://arxiv.org/abs/2104.14294>.
- Jia Deng, Wei Dong, Richard Socher, Li-Jia Li, Kai Li, and Li Fei-Fei. Imagenet: A large-scale hierarchical image database. In 2009 IEEE conference on computer vision and pattern recognition, pages 248–255. Ieee, 2009.
- Prafulla Dhariwal and Alexander Nichol. Diffusion models beat gans on image synthesis. Advances in neural information processing systems, 34:8780–8794, 2021.
- Weitao Feng, Wenbo Zhou, Jiyan He, Jie Zhang, Tianyi Wei, Guanlin Li, Tianwei Zhang, Weiming Zhang, and Nenghai Yu. Aqualora: Toward white-box protection for customized stable diffusion models via watermark lora. The International Conference on Machine Learning (ICML), 2024.
- Pierre Fernandez, Guillaume Couairon, Hervé Jégou, Matthijs Douze, and Teddy Furon. The stable signature: Rooting watermarks in latent diffusion models. International Conference on Computer Vision (ICCV), 2023.
- Pierre Fernandez, Hady Elsahar, I Zeki Yalniz, and Alexandre Mourachko. Video seal: Open and efficient video watermarking. arXiv preprint arXiv:2412.09492, 2024.
- Kaiming He, Xiangyu Zhang, Shaoqing Ren, and Jian Sun. Deep residual learning for image recognition. In IEEE / CVF Computer Vision and Pattern Recognition Conference (CVPR), pages 770–778, 2016.
- Jonathan Ho, Ajay Jain, and Pieter Abbeel. Denoising diffusion probabilistic models. Advances in neural information processing systems ((NeurIPS)), 2020.
- Edward J Hu, Yelong Shen, Phillip Wallis, Zeyuan Allen-Zhu, Yuanzhi Li, Shean Wang, Lu Wang, Weizhu Chen, et al. Lora: Low-rank adaptation of large language models. International Conference on Learning Representations (ICLR), 2022.
- Runyi Hu, Jie Zhang, Yiming Li, Jiwei Li, Qing Guo, Han Qiu, and Tianwei Zhang. Videoshield: Regulating diffusion-based video generation models via watermarking, 2025a. URL <https://arxiv.org/abs/2501.14195>.
- Xuming Hu, Hanqian Li, Jungang Li, Yu Huang, and Aiwei Liu. Videomark: A distortion-free robust watermarking framework for video diffusion models, 2025b. URL <https://arxiv.org/abs/2504.16359>.
- Yu Huang, Junhao Chen, Shuliang Liu, Hanqian Li, Qi Zheng, Yi R. Fung, and Xuming Hu. Video signature: In-generation watermarking for latent video diffusion models, 2025. URL <https://arxiv.org/abs/2506.00652>.
- Ziqi Huang, Yinan He, Jiashuo Yu, Fan Zhang, Chenyang Si, Yuming Jiang, Yuanhan Zhang, Tianxing Wu, Qingyang Jin, Nattapol Chanpaisit, Yaohui Wang, Xinyuan Chen, Limin Wang, Dahua Lin, Yu Qiao, and Ziwei Liu. VBench: Comprehensive benchmark suite for video generative models. In Proceedings of the IEEE/CVF Conference on Computer Vision and Pattern Recognition, 2024.
- MinHyuk Jang, Youngdong Jang, JaeHyeok Lee, Feng Yang, Gyeongrok Oh, Jongheon Jeong, and Sangpil Kim. Lvmark: Robust watermark for latent video diffusion models, 2025. URL <https://arxiv.org/abs/2412.09122>.
- Junjie Ke, Qifei Wang, Yilin Wang, Peyman Milanfar, and Feng Yang. Musiq: Multi-scale image quality transformer. In Proceedings of the IEEE/CVF international conference on computer vision, pages 5148–5157, 2021.

- Changhoon Kim, Kyle Min, Maitreya Patel, Sheng Cheng, and Yezhou Yang. Wouaf: Weight modulation for user attribution and fingerprinting in text-to-image diffusion models. In IEEE/CVF Conference on Computer Vision and Pattern Recognition (CVPR), 2024.
- Harold W. Kuhn. The hungarian method for the assignment problem. Naval Research Logistics Quarterly, 2:83–97, 1955. URL <https://onlinelibrary.wiley.com/doi/abs/10.1002/nav.3800020109>.
- Zhen Li, Zuo-Liang Zhu, Ling-Hao Han, Qibin Hou, Chun-Le Guo, and Ming-Ming Cheng. Amt: All-pairs multi-field transforms for efficient frame interpolation, 2023. URL <https://arxiv.org/abs/2304.09790>.
- Kepan Nan, Rui Xie, Penghao Zhou, Tiehan Fan, Zhenheng Yang, Zhijie Chen, Xiang Li, Jian Yang, and Ying Tai. Openvid-1m: A large-scale high-quality dataset for text-to-video generation. arXiv preprint arXiv:2407.02371, 2024.
- OpenAI. Video generation models as world simulators. <https://openai.com/index/video-generation-models-as-world-simulators/>, February 15 2024. [Technical report].
- William Peebles and Saining Xie. Scalable diffusion models with transformers. In Proceedings of the IEEE/CVF international conference on computer vision, pages 4195–4205, 2023.
- Alec Radford, Jong Wook Kim, Chris Hallacy, Aditya Ramesh, Gabriel Goh, Sandhini Agarwal, Girish Sastry, Amanda Askell, Pamela Mishkin, Jack Clark, et al. Learning transferable visual models from natural language supervision. In International conference on machine learning, pages 8748–8763. PMLR, 2021.
- Bram Rijsbosch, Gijs van Dijck, and Konrad Kollnig. Adoption of watermarking measures for ai-generated content and implications under the eu ai act. arXiv preprint arXiv:2503.18156, 2025.
- Robin Rombach, Andreas Blattmann, Dominik Lorenz, Patrick Esser, and Björn Ommer. High-resolution image synthesis with latent diffusion models. In IEEE/CVF conference on computer vision and pattern recognition (CVPR), 2022.
- Olaf Ronneberger, Philipp Fischer, and Thomas Brox. U-net: Convolutional networks for biomedical image segmentation. In Medical image computing and computer-assisted intervention (MICCAI), 2015.
- Aniruddha Saha, Akshayvarun Subramanya, and Hamed Pirsiavash. Hidden trigger backdoor attacks. In AAAI Conference on Artificial Intelligence, 2020.
- Jiaming Song, Chenlin Meng, and Stefano Ermon. Denoising diffusion implicit models. arXiv preprint arXiv:2010.02502, 2020.
- Jiuniu Wang, Hangjie Yuan, Dayou Chen, Yingya Zhang, Xiang Wang, and Shiwei Zhang. Modelscope text-to-video technical report. arXiv preprint arXiv:2308.06571, 2023.
- Yuxin Wen, John Kirchenbauer, Jonas Geiping, and Tom Goldstein. Tree-ring watermarks: Fingerprints for diffusion images that are invisible and robust. arXiv preprint arXiv:2305.20030, 2023.
- Zijin Yang, Kai Zeng, Kejiang Chen, Han Fang, Weiming Zhang, and Nenghai Yu. Gaussian shading: Provable performance-lossless image watermarking for diffusion models. In IEEE/CVF Conference on Computer Vision and Pattern Recognition (CVPR), 2024.
- Richard Zhang, Phillip Isola, Alexei A Efros, Eli Shechtman, and Oliver Wang. The unreasonable effectiveness of deep features as a perceptual metric. Proceedings of the IEEE Conference on Computer Vision and Pattern Recognition, 2018.

A Datasets and training

We train on 10,000 videos from OpenVid-1M [Nan et al. \(2024\)](#) using AdamW ($\beta_1=0.9$, $\beta_2=0.999$, weight decay 10^{-2}), learning rate 10^{-4} , batch size 1 on 1 NVIDIA A6000 GPU, for 6000 steps. Training uses 8-frame clips at 256 resolution. At test time, we evaluate full-length generations (25 frames for SVD-XT and 16 frames for MS).

B Computational cost

Training takes ≈ 8 GPU hours. Only one basis per block is active at inference, so the decoding cost matches a single rank- r low-rank update per targeted block. The added parameters are ≈ 2 M. Empirically, this adds $<5\%$ to the decoding time versus the frozen decoder.

C Generation Quality Evaluation Metrics

Subject Consistency (SC). For a video with frames $1, \dots, T$, let d_t be the L2-normalized DINO ([Caron et al., 2021](#)) image feature of frame t . SC averages the cosine similarity of each frame to (i) the first frame and (ii) its previous frame:

$$S_{\text{SC}} = \frac{1}{T-1} \sum_{t=2}^T \frac{1}{2} (\langle d_1, d_t \rangle + \langle d_{t-1}, d_t \rangle).$$

Background Consistency (BC). Let c_t be the L2-normalized CLIP image feature of frame t . BC mirrors SC but uses CLIP features ([Radford et al., 2021](#)):

$$S_{\text{BC}} = \frac{1}{T-1} \sum_{t=2}^T \frac{1}{2} (\langle c_1, c_t \rangle + \langle c_{t-1}, c_t \rangle).$$

Motion Smoothness (MS). Drop the odd frames to form a lower-FPS sequence and synthesize them with a video frame-interpolation model (AMT) ([Li et al., 2023](#)). For each removed frame f_{2t-1} with interpolation \hat{f}_{2t-1} , compute the mean absolute error (MAE). The raw error is then normalized to $[0, 1]$ (same normalization as the flicker metric):

$$E = \frac{1}{T/2} \sum_{t=1}^{T/2} \text{MAE}(\hat{f}_{2t-1}, f_{2t-1}), \quad S_{\text{MS}} = \frac{255 - E}{255}.$$

Imaging Quality (IQ). Per frame, run the MUSIQ ([Ke et al., 2021](#)) image-quality predictor (0–100), then average over frames and linearly rescale:

$$S_{\text{IQ}} = \frac{1}{T} \sum_{t=1}^T \frac{\text{MUSIQ}(t)}{100}.$$

D Robustness and Attack Protocol

We evaluate SPDMark across photometric, temporal, and post-processing attacks.

Photometric and Spatial Attacks. We simulate common visual distortions encountered during content sharing: **Gaussian Noise:** Additive noise $\mathcal{N}(0, \sigma^2)$ with $\sigma = 0.05$ (SNR ≈ 26 dB), simulating sensor noise or low-light capture. **Gaussian Blur:** 7×7 convolution with $\sigma = 1.5$, approximating defocus or motion

blur. **Rotation:** Random rotation $\theta \in [-15, +15]$ with bicubic interpolation, followed by center crop to original dimensions. **Center Crop:** Extract the central 90% region ($0.95\times$ scaling), then resize it back to the original resolution. **Rescale:** Downsample by $0.5\times$ using bicubic interpolation, then upsample back (lossy cycle common in social media). **Color Jitter:** Random brightness and contrast adjustments within $\pm 10\%$, common in auto-enhancement filters. **Text Overlay:** Add semi-transparent captions using (40pt font, 50% opacity, bottom 20% of frame), simulating subtitles or watermark overlays. We chose moderate attack strengths representative of real-world degradation. For example, $\sigma = 0.05$ noise is perceptible but not destructive. Stronger attacks would make content unusable regardless of watermarking.

Post-Processing and Screen Recording Simulation. We include transformations approximating recompression pipelines and phone screen capture: **Multi-Stage Recompression:** Two-pass encoding: (1) H.264 at CRF=28, (2) decode and re-encode with H.265 (libx265) at a target bitrate of 600 kbps. Simulates upload \rightarrow platform transcode \rightarrow download cycle. **Screen Recording:** Approximate phone camera capture of screen playback by the following steps: downscale to 70% resolution and upscale back (resolution loss), then add Gaussian noise ($\sigma = 0.03$) for sensor artifacts, then apply mild vignetting (20% intensity reduction at corners), then add defocus blur (3×3 Gaussian kernel, $\sigma = 0.8$), finally recompression at 600 kbps. **Denoising:** Apply bilateral filter (spatial $\sigma=3$, intensity $\sigma=50$) combined with affine jitter (± 3 pixels translation per frame), simulating video stabilization post-processing that smooths content while introducing slight geometric shifts.

Temporal Attacks. To evaluate temporal integrity and forensic capabilities: **Frame Drop:** Randomly delete 50% of frames uniformly, creating temporal gaps. **Frame Swap (Random):** Apply random permutation to all frames, destroying temporal order. **Frame Swap (Adjacent):** Swap adjacent pairs $(t, t + 1) \leftrightarrow (t + 1, t)$ for 30% of consecutive pairs. **Frame Insert:** Duplicate 20% of frames at random positions or inject Gaussian noise frames. **Video Trim:** Remove first and last 20% of frames (cut intro/outro).

E Additional Qualitative Examples

Figures 4 (SVD) and 5 (ModelScope) provide extended visualisations. For each base model, we show three videos and, for each video, display seven consecutive frames from the non-watermarked video followed by the corresponding SPDMark sample of the same video. textttSPDMark closely tracks the clean videos: textures, edges, and colors remain visually consistent, and we do not observe watermark-induced artifacts. The sequences further indicate that temporal coherence is preserved.

E.1 Sampling Configuration on ModelScope

Setup. We ablate three factors for ModelScope (Table 5): number of generated frames, diffusion steps, and CFG. For each configuration, we use the same prompt set and seed protocol as in the main results, and report Bit accuracy, Robust accuracy, and Video quality metrics. The results mirror those of SVD-XT: longer videos improve robust accuracy, while diffusion steps and guidance have a limited effect on extraction or video quality.

SVD

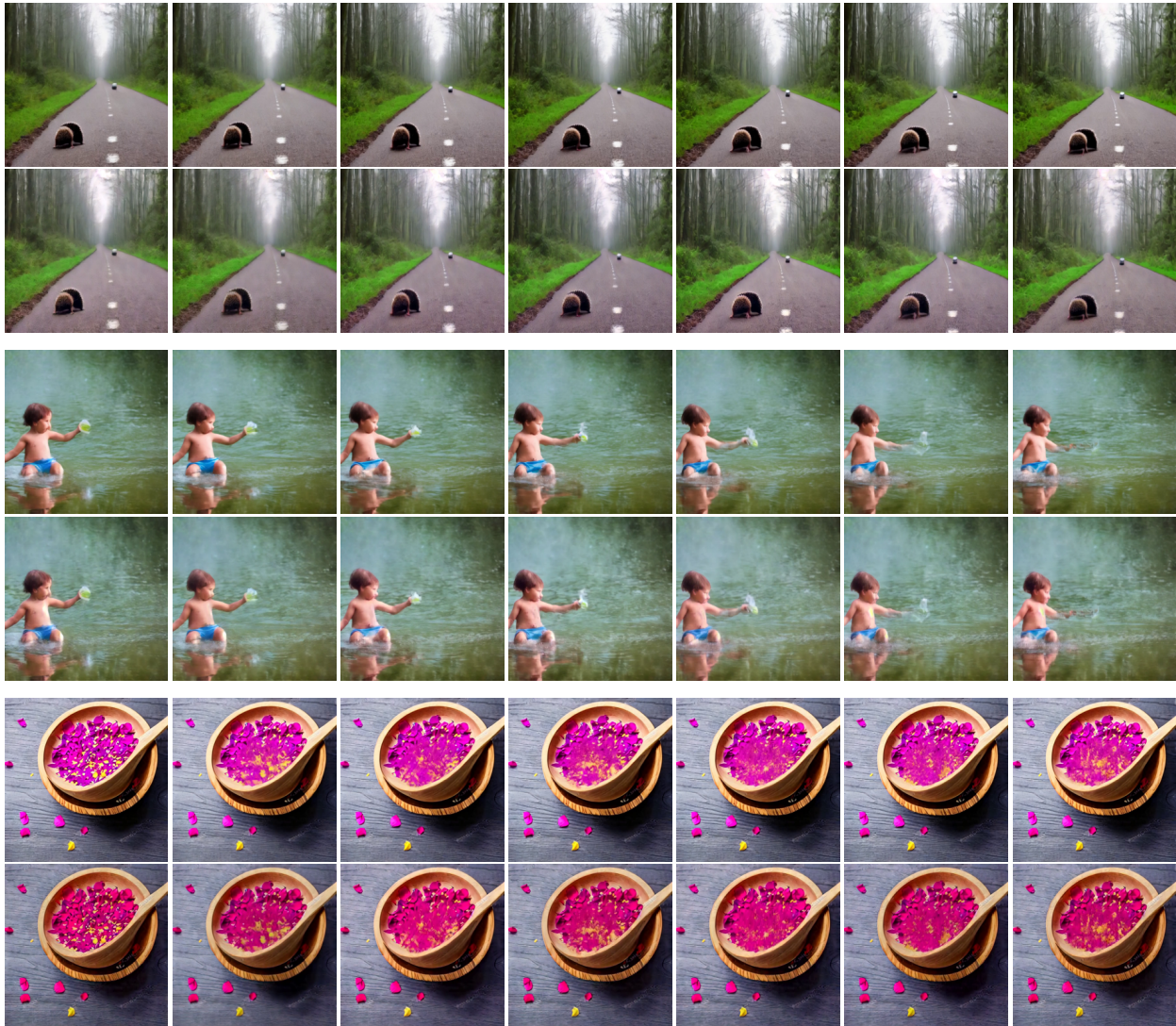


Figure 4: SVD videos: Seven frames per row. For each video, the No watermark row is followed by the corresponding SPDMark row (for the same video).

Table 5: Sampling and ablation studies on **ModelScope**. Robust means bit accuracy under the attack suite used.

| Factor | Setting | Bit Acc \uparrow | Robust | SC \uparrow | BC \uparrow | MS \uparrow | IQ \uparrow |
|----------|---------|--------------------|--------------|---------------|---------------|---------------|---------------|
| Frames | 8 | 0.955 | 0.889 | 0.964 | 0.974 | 0.974 | 0.480 |
| | 25 | 0.989 | 0.916 | 0.851 | 0.920 | 0.948 | 0.468 |
| Steps | 10 | 0.983 | 0.910 | 0.881 | 0.933 | 0.974 | 0.458 |
| | 25 | 0.983 | 0.910 | 0.898 | 0.945 | 0.967 | 0.500 |
| Guidance | 6 | 0.987 | 0.914 | 0.908 | 0.944 | 0.967 | 0.513 |
| | 12 | 0.988 | 0.915 | 0.911 | 0.945 | 0.964 | 0.510 |

ModelScope

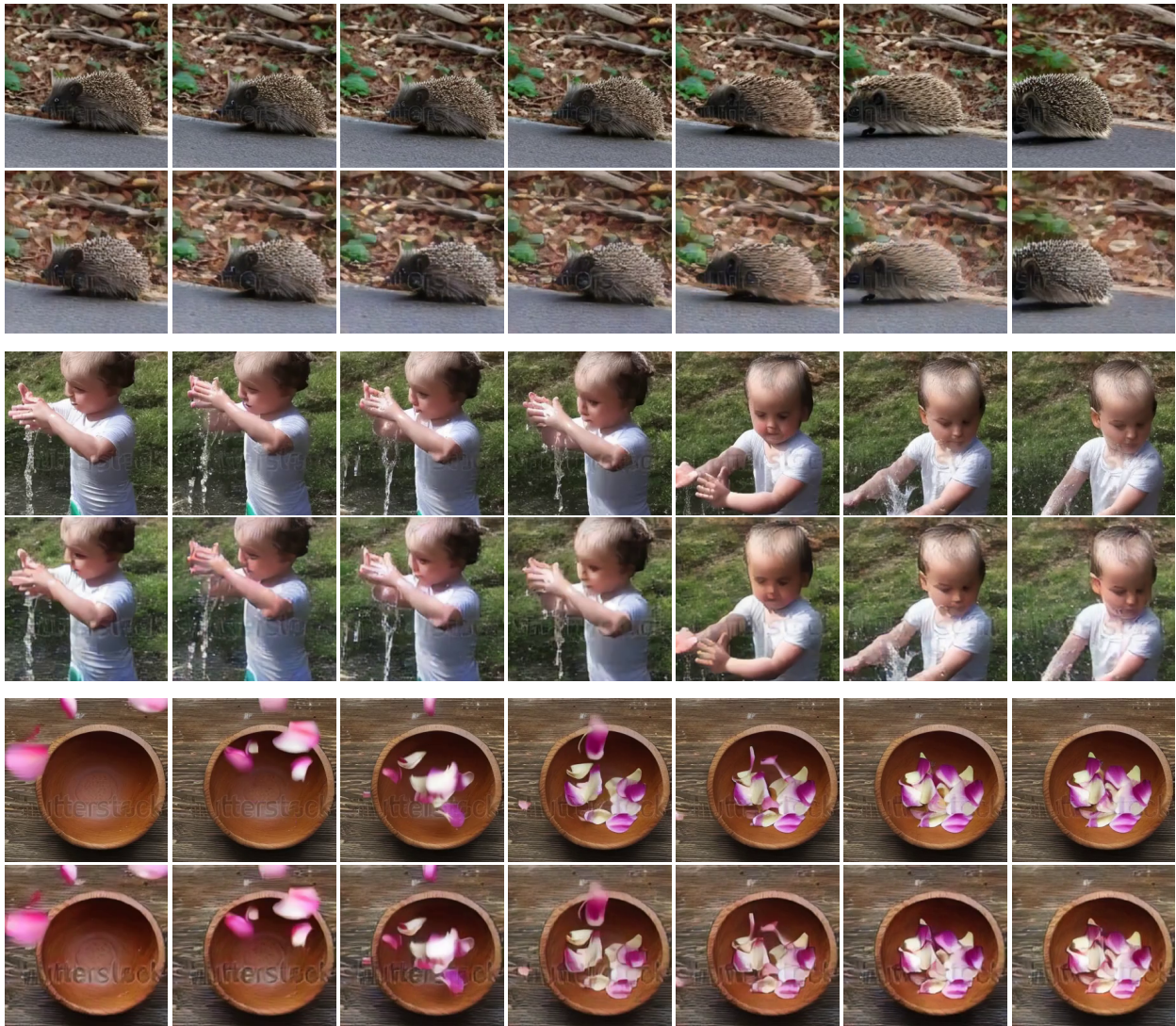


Figure 5: ModelScope videos: Seven frames per row. For each video, the No watermark row is followed by the corresponding SPDMark row (for the same video).